

Differential Blocking Effects of the Acetaldehyde-derived DNA Lesion N^2 -Ethyl-2'-deoxyguanosine on Transcription by Multisubunit and Single Subunit RNA Polymerases^{*[5]}

Received for publication, May 29, 2008, and in revised form, July 31, 2008. Published, JBC Papers in Press, July 31, 2008, DOI 10.1074/jbc.M804086200

Tsu-Fan Cheng[‡], Xiaopeng Hu[§], Averell Gnatt[§], and Philip J. Brooks^{‡1}

From the [‡]Section on Molecular Neurobiology, Laboratory of Neurogenetics, National Institute on Alcohol Abuse and Alcoholism, Bethesda, Maryland 20892 and the [§]Department of Pharmacology and Experimental Therapeutics, University of Maryland School of Medicine, Baltimore, Maryland 21201

Acetaldehyde, the first metabolite of ethanol, reacts with DNA to form adducts, including N^2 -ethyl-2'-deoxyguanosine (N^2 -Et-dG). Although the effects of N^2 -Et-dG on DNA polymerases have been well studied, nothing is known about possible effects of this lesion on transcription by RNA polymerases (RNAPs). Using primer extension assays *in vitro*, we found that a single N^2 -Et-dG lesion is a strong block to both mammalian RNAPII and two other multisubunit RNAPs, (yeast RNAPII and *Escherichia coli* RNAP), as well as to T7 RNAP. However, the mechanism of transcription blockage appears to differ between the multisubunit RNAPs and T7 RNAP. Specifically, all three of the multisubunit RNAPs can incorporate a single rNTP residue opposite the lesion, whereas T7 RNAP is essentially unable to do so. Using the mammalian RNAPII, we found that CMP is exclusively incorporated opposite the N^2 -Et-dG lesion. In addition, we also show that the accessory transcription factor TFIIS does not act as a lesion bypass factor, as it does for other nonbulky DNA lesions; instead, it stimulates the polymerase to remove the CMP incorporated opposite the lesion by mammalian RNAPII. We also include models of the N^2 -Et-dG within the active site of yeast RNAPII, which are compatible with our observations.

Acetaldehyde (ACD)² is a genotoxin, known animal carcinogen, and suspected human carcinogen (1, 2). Although small amounts of ACD are produced endogenously during threonine catabolism (3), the most significant source of human exposure to ACD is via the metabolism of ethanol. In the human body, ethanol is first converted to ACD via the enzyme alcohol dehydrogenase, and ACD is further converted to acetate via aldehyde dehydrogenase (ALDH), primarily by the hepatic enzyme

ALDH2. Approximately 50% of East Asian individuals are deficient in ALDH2 activity because of an amino acid substitution resulting in an inactive enzyme (4). ALDH2-deficient individuals are at a substantially elevated risk of esophageal cancer when they drink heavily, and other mechanistic evidence indicates that ACD is responsible for the increased cancer risk (2).

Several studies have shown that ACD can react with DNA to form adducts (5–12). One of the first identified and most well studied ACD-derived lesions is N^2 -ethyl-2'-deoxyguanosine (N^2 -Et-dG) (Fig. 1). N^2 -Et-dG is the stable form of N^2 -Eti-dG, the immediate product of the ACD reaction with dG. In the presence of basic compounds such as histones and polyamines, ACD can also give rise to other DNA adducts (13, 14). Elevated levels of these ACD-related DNA adducts, including N^2 -Et-dG, have been observed in white blood cell DNA in humans following alcohol consumption, with significantly higher levels observed in ALDH2-deficient individuals (15). Thus, the biological effects of these DNA lesions are of potential clinical relevance.

In view of the relationship between alcohol and cancer, the effect of N^2 -Et-dG on DNA replication and mutagenesis have been well studied. N^2 -Et-dG is a strong block to DNA polymerase α (16) but is efficiently bypassed by the replicative polymerase δ (17) (see also Ref. 18). No published data are available for this lesion with the replicative polymerase ϵ . In addition, cells have specialized DNA polymerases that can bypass N^2 -Et-dG in an error-free manner (16, 19, 20). In human cells *in vivo*, the major genotoxic effects of the lesion appear to be the result of replication blockage, with some capacity for generating mutations including single base deletions and transversions (21).

In contrast to the effect on DNA polymerases, no studies have been done to examine the effects of this lesion on transcription by RNA polymerases (RNAPs). Therefore, in the present work we investigated the effects of N^2 -Et-dG on transcription by mammalian RNAPII, as well as two other multisubunit RNAPs, yeast RNAPII and *Escherichia coli* RNAP. To address the possibility of bypass factors, we also tested the effect of the transcription factor TFIIS, which has been recently shown to stimulate lesion bypass during transcription past the oxidized guanosine lesion 8-oxo-dG (22, 23), to allow mammalian RNAPII to bypass N^2 -Et-dG.

As noted above, ALDH2 plays a key role on the metabolism of ACD. Because ALDH2 is localized to the mitochondria (4), it follows that ACD formed from ethanol metabolism must be

* This work was supported by the Division of Clinical and Intramural Research, National Institute on Alcohol Abuse and Alcoholism. The costs of publication of this article were defrayed in part by the payment of page charges. This article must therefore be hereby marked "advertisement" in accordance with 18 U.S.C. Section 1734 solely to indicate this fact.

[5] The on-line version of this article (available at <http://www.jbc.org>) contains supplemental Fig. S1 and supplemental text.

¹ To whom correspondence should be addressed: Section on Molecular Neurobiology, Laboratory of Neurogenetics, National Institute on Alcohol Abuse and Alcoholism, 5625 Fishers Ln., Rm. 3S-32, Rockville, MD 20852. Tel.: 301-496-7920; Fax: 301-480-2839; E-mail: pjbrooks@mail.nih.gov.

² The abbreviations used are: ACD, acetaldehyde; N^2 -Et-dG, N^2 -ethyl-2'-deoxyguanosine; RNAP, RNA polymerase; ALDH, aldehyde dehydrogenase.

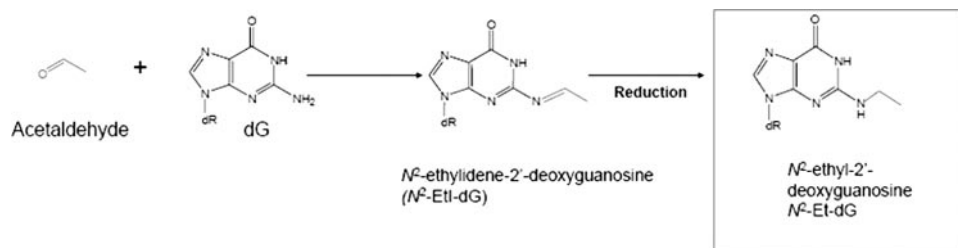


FIGURE 1. **Formation of N^2 -Et-dG by the reaction of acetaldehyde and guanosine.** The initial reaction product is N^2 -Etl-dG, which undergoes a reduction reaction to yield the stable DNA lesion N^2 -Et-dG, which was used in the experiments reported here.

able to enter mitochondria to be a substrate for the enzyme. As a result, it is likely that, especially in ALDH2-deficient individuals, ACD adduction of hepatic mitochondrial DNA could be significant. Therefore, in addition to investigating the effect of N^2 -Et-dG on transcription by RNAPII, we also examined the effect of the lesion on transcription by T7RNAP, as a model for mitochondrial RNAP. Eukaryotic mitochondrial RNAPs are single subunit polymerases that are highly homologous to T7 and other single subunit phage polymerases, especially in the residues and overall structure of the active site (24).

We found that a single N^2 -Et-dG lesion is a strong block to both mammalian and other multisubunit RNAPII, as well as to T7 RNAP. Interestingly, however, all three of the multisubunit RNAPs can incorporate a single rNTP residue opposite the lesion, whereas T7 RNAP is unable to do so. Using the mammalian RNAPII, we found that CMP is exclusively incorporated opposite the N^2 -Et-dG lesion. We also show that the accessory transcription factor TFIIS does not act as a lesion bypass factor, as it does for other nonbulky DNA lesions; instead, it stimulates the polymerase to remove the CMP incorporated opposite the lesion.

MATERIALS AND METHODS

Oligonucleotide Synthesis—A phosphoramidite containing N^2 -Et-dG was synthesized by Glen Research (Sterling, VA). Oligonucleotides containing the lesion were synthesized on an ABI DNA synthesizer using standard chemistry and deprotection and purified by denaturing PAGE.

The sequence of the DNA template strand used in the *in vitro* transcription was: 5'-CATGCTGATGAATTCCTTCNCTA-CCTTCCTCTCCATTT-3'. The underlined N indicates the position of either deoxyguanosine or the N^2 -Et-dG.

High pressure liquid chromatography-purified RNA primers were obtained from IDT (Coralville, IA). The sequence of the RNA oligonucleotide used for running start transcription was 5'-AGAGGAAAGU-3', and that for standing start transcription was 5'-AGGAAAGUAG-3'. The sequence of the 30-mer RNA marker was 5'-UAGGUUCCACCUUACCAGCCUU-UUACAGAU-3'.

RNA Primer Labeling with [γ - 32 P]ATP by T4 Polynucleotide Kinase—RNA primers were labeled with 30 μ Ci of [γ - 32 P]ATP (PerkinElmer Life Sciences) at 5' end by T4 polynucleotide kinase (New England Biolabs). The reaction was carried out at 37 °C for 30 min and heat-inactivated at 65 °C for 15 min. The unincorporated nucleotides were removed by NucAway

spin column (Ambion, TX) according to the manufacturer's instructions.

Proteins—Mammalian RNAPII (from calf thymus) and yeast RNAPIIs were purified as described (25). Full-length N-terminal histidine-tagged human TFIIS was expressed in the bacterial expression vector pET21 in BL-21 cells (Invitrogen). TFIIS was purified by nickel-nitrilotriacetic acid affinity chromatography as per company recommendations (Qiagen), followed by a final column employing MonoS (Bio-Rad) (supplemental Fig. S1). *E. coli* RNAP and T7 RNAP were purchased from Epicenter (Madison, WI).

In Vitro Transcription—The methodology for analyzing the effects of DNA lesions on transcription was based on the direct assembly of transcription elongation complexes introduced by Kashlev and co-workers (26). The single-stranded DNA template was used at 2 μ M, and mixed with the RNA primer (2 μ M) in the reaction buffer specific for each polymerase. The amount of RNA primer used assumed complete recovery after the spin column purification step. Mammalian RNAPII buffer was: 50 mM Tris-HCl (pH 7.6), 10 mM dithiothreitol, 6 mM MgCl₂ and 40 mM (NH₄)₂SO₄. The same buffer was also used for yeast RNAPII. *E. coli* RNAP reaction buffer was 20 mM HEPES (pH 7.9), 40 mM KCl, and 5 mM MgCl₂. T7 RNAP reaction buffer was 20 mM HEPES (pH 7.9), 10 mM magnesium acetate, 20 mM sodium acetate, 1 mM dithiothreitol, and 0.1 mM EDTA.

To set up the reactions, 1 μ l of RNA primer (2 pmol) was annealed to the template in a volume of 8 μ l by first heating the mixture to 45 °C for 5 min and then cooled to room temperature (approximately 24 °C) 2 °C every 2 min (26). Then 1 μ l of a 1.13 μ M solution of mammalian RNAPII or yeast RNAPII was added to the reaction and incubated for 10 min at room temperature. These conditions give a nominal molar ratio of primer:template to polymerase of \approx 2. For the prokaryotic enzymes, the reactions contained 10 units (1 μ l) of *E. coli* RNAP or 50 units (1 μ l) of T7 RNAP.

In vitro transcription was started by adding the indicated ribonucleotide(s) (final concentration, 100 μ M) and stopped by removing samples and mixing with 2 \times formamide gel loading dye (95% (v/v) formamide, 0.25% (w/v) bromphenol blue, 0.025% (w/v) xylene cyanol, and 5 mM EDTA, pH 8.0) at the specific time points. The transcription products were separated on 20% acrylamide, 7 M urea gels and detected by autoradiography.

Quantitative Analysis of Apparent K_m Values—The apparent K_m is the concentration of NTP at which the rate of incorporation opposite dG or N^2 -Et-dG is half-maximal during a fixed reaction time (27). To determine the apparent K_m values for CTP incorporation opposite dG or N^2 -Et-dG, standing start experiments were performed with varying concentrations of CTP as shown in Fig. 3, with incubation for 20 min at 25 °C. The resulting gels were dried, and the results were quantified using a Typhoon Imager (Molecular Dynamics), with subtraction of the background values at time 0 (27). Apparent K_m values were

Acetaldehyde DNA Lesion Blocks Transcription

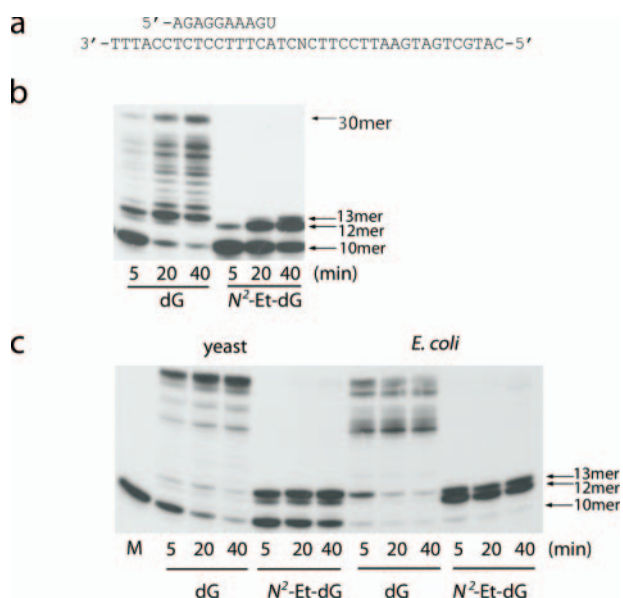


FIGURE 2. *N*²-Et-dG is a strong block to transcription by multisubunit RNAPs. *a*, diagram of the 10-mer RNA primer (top strand) annealed to a 38-mer DNA template (bottom strand). The *N* represents either guanine or *N*²-Et-dG lesion. *b*, a running start study using mammalian RNAP II. Transcription was initiated by the addition of rNTPs (100 μ M each), and samples were analyzed at the indicated times. Transcription on the *N*²-Et-dG lesion-containing template was blocked after inserting one nucleotide (13-mer). *c*, running start studies with either yeast RNAPII or *E. coli* RNAP. Both enzymes are able to incorporate a nucleotide opposite the *N*²-Et-dG, as indicated by the accumulation of the 13-mer.

obtained by nonlinear curve fitting using GraphPad Prism. The values given are the means \pm S.E., based on two independent determinations.

RESULTS

*N*²-Et-dG Is a Strong Block to Transcription Elongation by Mammalian RNAPII—To study the effects of *N*²-Et-dG on transcription, we utilized a primer extension assay, in which an RNA primer is first annealed to a lesion-containing or control (lesion-free) oligonucleotide DNA template. RNAP is then added, and transcription is initiated by the addition of rNTPs. This strategy is adapted from the methodology of Kashlev and co-workers (26) and is analogous to the methodology used to study the effects of DNA lesions on DNA polymerases (16, 19, 20). During transcription by RNAPs under these conditions, the nontemplate DNA strand is not required for transcription (26, 29, 30), and the absence of the nontemplate strand does not affect the stability of eukaryotic RNAPII transcription elongation complexes (31).

In our initial experiments, we used a “running start” set-up in which a 10-mer primer was annealed to a 38-mer DNA template two nucleotides 3' to the lesion (Fig. 2*a*). As shown in Fig. 2*b*, the *N*²-Et-dG lesion poses as a strong blockage for transcription by calf RNAPII. Over time, a slow incorporation of nucleotides opposite the lesion base is observed.

We repeated these experiments using two other purified multisubunit RNAPs. As shown in Fig. 2*c*, similar to the results using mammalian RNAPII, both yeast RNAPII and *E. coli* RNAP were also able to incorporate a single nucleotide opposite the *N*²-Et-dG lesion before stalling. Also, in contrast to

mammalian RNAPII, with these enzymes, a minimal amount of bypass product was observable.

Inspection of the results shown in Fig. 2*c* indicated that the three polymerases differ in their ability to incorporate a nucleotide opposite the lesion. These differences are illustrated by comparing the relative amount of the 13-mer band (which represents nucleotide incorporation opposite the lesion) to the 12-mer, which represents transcription up to the site of the lesion. Because the 12-mer band is by definition the result of active polymerization, the relative amount of the 13-mer band to the 12-mer band is a measure of the fraction of active polymerases that were able to incorporate nucleotide opposite the lesion.

From the results shown in Fig. 2 as well as other analyses (not shown) the 13-mer/12-mer ratio at the 40-min time point for the yeast polymerase is 2.7–4.5, compared with 0.34–0.83 for the calf polymerase and 0.6–0.85 for the *E. coli* polymerase. On the basis of these differences, as well as the faster time course of nucleotide incorporation opposite the lesion for the *E. coli* polymerase compared with the calf (Fig. 2), our results indicate that the ability to incorporate nucleotide opposite the *N*²-Et-dG lesion is highest for yeast RNAPII, followed by the *E. coli* RNAP and then the calf RNAPII.

It should be noted that using the 13-mer/12-mer ratio as a basis for comparison normalizes for any variation in amount of transcription in different samples. Such variation, which is seen in Figs. 2 and 5, may be due to differences in the number of active polymerase molecules in a given enzyme preparation and/or to the efficiency of formation of the primer-template-enzyme complexes.

Together, our results show that under running start conditions, the *N*²-Et-dG lesion is a very strong block to transcription elongation by mammalian RNAP II, as well as yeast RNAPII and *E. coli* RNAP. All three multisubunit polymerases are able to incorporate nucleotide opposite the lesion, prior to stalling, although the ability to incorporate nucleotide opposite the lesion varies between the three enzymes.

Mammalian RNAP II Incorporates CMP Opposite N²-Et-dG during Transcription—We next carried out a standing start RNA extension study using mammalian RNAPII with template containing either dG or *N*²-Et-dG as the first template base to be transcribed. Fig. 3*b* shows that under standing start conditions, mammalian RNAPII was also able to slowly incorporate a single nucleotide opposite the lesion before stalling, consistent with the running start results.

In Fig. 3*b*, we note that a limited degree of read-through product beyond the lesion site is clearly observable, in contrast to the results with the running start set-up (Fig. 2*b*). Because the template is identical in both cases, but the primer is annealed to different locations in the running start *versus* the standing start experiments, the difference between the two is most likely due in part to different initial RNAPII/nucleic acid structures. Such an interpretation is fully compatible with previous findings (32). The difference may also reflect differences in the number of possible configurations that the ethyl group can assume in the running *versus* standing start modes, an issue we will return to under “Discussion.” The important point here is that the results from the running and standing start experiments are in

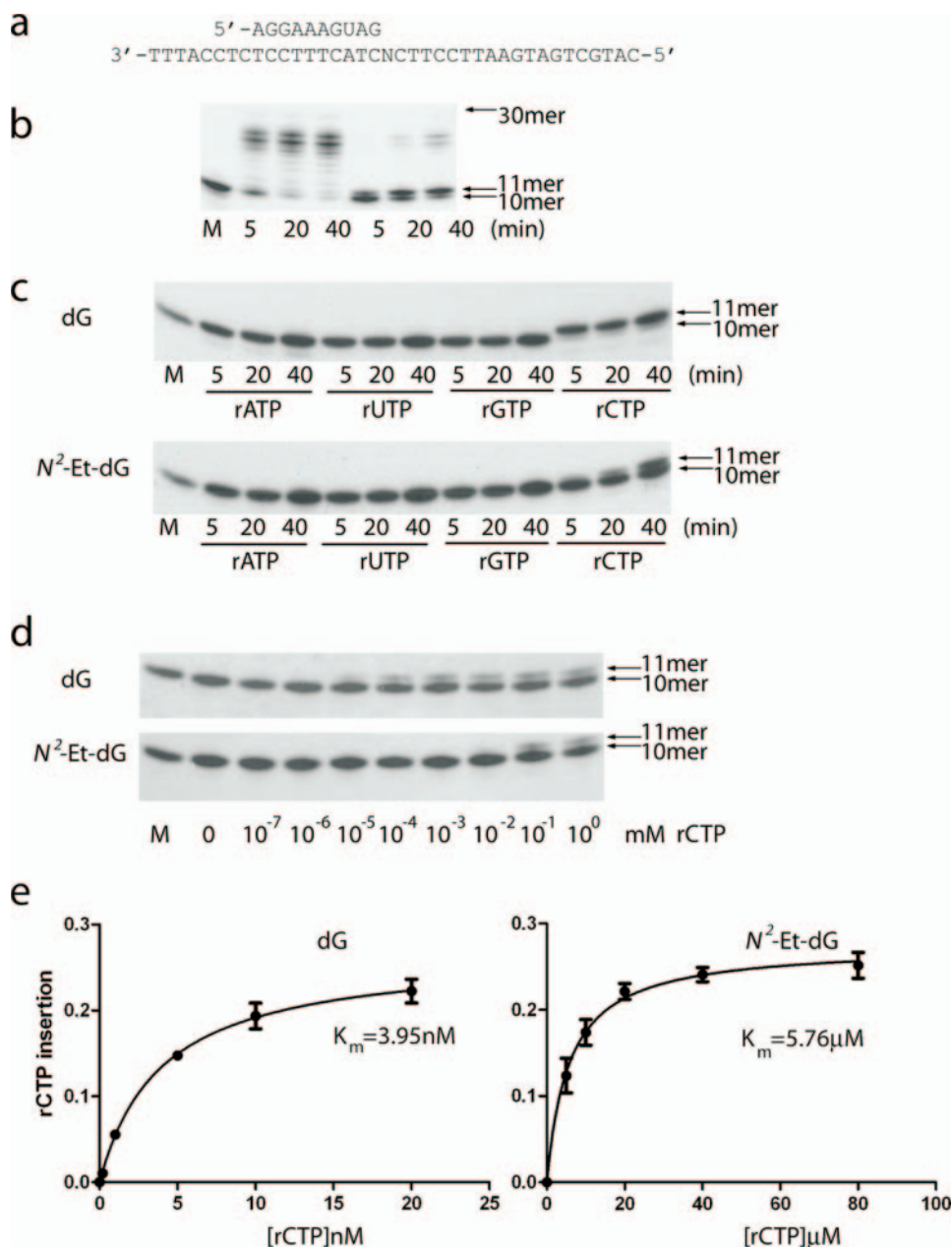


FIGURE 3. N^2 -Et-dG is a strong block to transcription in the standing start reaction. *a*, a 10-mer RNA oligonucleotide (top strand) annealed to the same DNA template (bottom strand). *N* indicates either guanine or N^2 -Et-dG. *b*, mammalian RNAPII transcription on either control or lesion template. Only one nucleotide insertion was detected on the lesion template (11-mer). *c*, individual nucleotides ($100 \mu\text{M}$ each) were added to the standing start reactions, and samples collected at the indicated times. CMP was incorporated by mammalian RNAPII opposite the lesion. *d*, mammalian RNAPII was incubated with increasing concentrations of CTP for 20 min, and the amount of extended primer on either the control or N^2 -Et-dG containing template was determined. Representative results are shown; the values from duplicate experiments were quantified, and the values are reported in the text. *e*, quantitative analysis of additional incorporation experiments using restricted ranges of CTP concentration. The curves were generated using nonlinear regression analysis (GraphPad Prism), and the resulting apparent K_m values are indicated. The data points are the means \pm S.E. of duplicate determinations.

agreement in that in both conditions, the polymerase is able to slowly incorporate 1 nucleotide opposite the lesion.

To determine which nucleotide was incorporated opposite the N^2 -Et-dG lesion, the standing start RNA extension study was conducted as in Fig. 3*b*, but with each of the four ribonucleotides added separately at a concentration of $100 \mu\text{M}$. As expected, under these conditions, mammalian RNAPII prefers

to incorporate CMP opposite the unmodified template dG (Fig. 3*c*). With N^2 -Et-dG lesion as the template, only cytosine incorporation was observed, although clearly more slowly than with a template dG (Fig. 3*d*). These results suggest that Watson-Crick base pairing specificity was still preserved during nucleotide incorporation opposite N^2 -Et-dG.

To quantify the magnitude of the effect of the lesion on nucleotide incorporation, we determined the concentration of NTP at which the rate of incorporation opposite dG or N^2 -Et-dG is half-maximal during a fixed reaction time (27). This value, the apparent K_m , has been used by other workers to compare the relative rates of nucleotide incorporation by RNAPs under various experimental conditions (27, 33). Representative data from these initial experiments, which used a wide range of CTP concentrations, are shown in Fig. 3*d*. Based on these analyses, the apparent K_m for CTP incorporation opposite template dG was in the low nanomolar range, in good agreement with the apparent K_m values obtained by Kornberg and co-workers (27) for yeast RNA-P II using a similar analysis. In contrast, with the N^2 -Et-dG template, the apparent K_m for CTP incorporation was in the low micromolar range.

To increase the accuracy of our apparent K_m determinations, we carried out additional experiments using a smaller range of CTP concentrations around the apparent K_m values predicted for the dG and N^2 -Et-dG templates based on the initial analysis. As shown in Fig. 3*e*, these experiments gave an apparent K_m for CTP incorporation opposite template dG of 3.95 nM, compared with $5.76 \mu\text{M}$ for the N^2 -Et-dG template, indicating that the N^2 -Et-dG

reduces CTP incorporation by ≈ 1500 -fold.

TFIIS Does Not Stimulate Transcription Past the N^2 -Et-dG Lesion—The general transcription elongation factor TFIIS is known for its role in stimulating the arrested RNAPII to cleave the nascent mRNA during transcription (34, 35). This generates a new 3' end that allows transcription to resume. On helix-distorting DNA lesions such as a cyclobutane py-

Acetaldehyde DNA Lesion Blocks Transcription

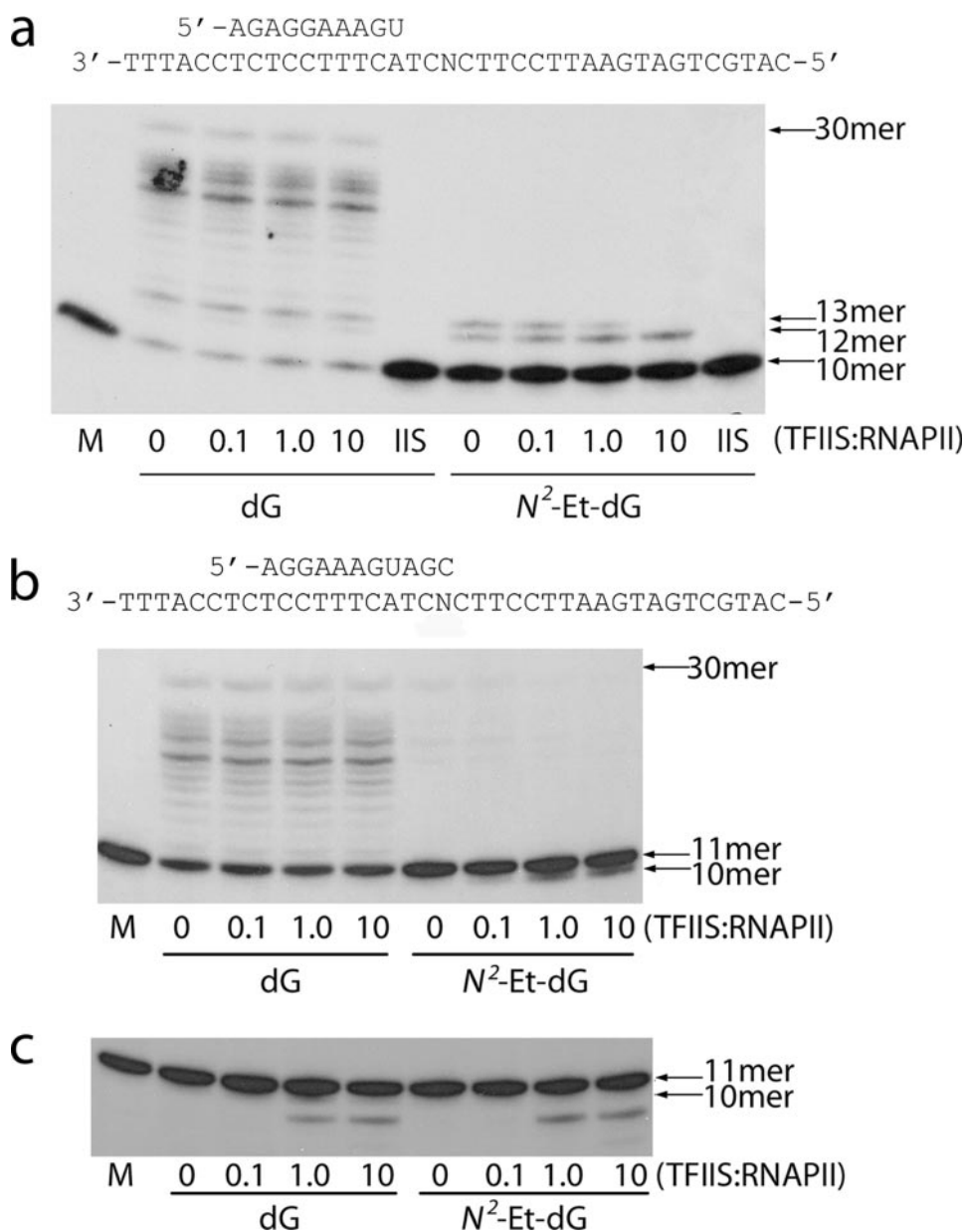


FIGURE 4. TFIIS is not a transcription bypass factor for mammalian RNAPII at the *N*²-Et-dG lesion. *a*, TFIIS was added to the running start reaction at increasing concentrations. The nucleotide opposite the lesion is removed when TFIIS is presented at the higher concentration (1.0- and 10-fold). Samples in lanes marked *IIS* were incubated with the amount of TFIIS used in the 10-fold ratio lanes but no RNAPII. *b*, a 11-mer RNA primer is annealed to the template, where a cytosine on the 3' end is opposite either a guanine or a *N*²-Et-dG lesion base. *c*, increasing concentrations of TFIIS stimulate transcript cleavage by 2 nucleotides with either the dG or *N*²-Et-dG template. All of the incubations were for 40 min.

rimidine dimer, the addition of TFIIS stimulates the polymerase stalled at the lesion to backtrack (36, 37). In contrast, other data indicate that TFIIS can act as a bypass factor by stimulating transcription past nonbulky DNA lesions such as 8-oxo-dG (22, 23).

To investigate whether TFIIS can affect the ability of mammalian RNAPII to bypass *N*²-Et-dG, we first carried out a running start experiment similar to that described above (Fig. 2), including increasing amounts of TFIIS (Fig. 4*a*). This condition is most analogous to the *in vivo* situation, in which transcription takes place in the presence of rNTPs and TFIIS is present.

When the template with *N*²-Et-dG lesion was transcribed in the absence of TFIIS, mammalian RNAPII alone was able to incorporate some nucleotide opposite the lesion, consistent with the results shown in Fig. 2*b*. However, with increasing TFIIS concentrations, the band corresponding to nucleotide incorporation opposite the lesion was reduced and completely abolished at high TFIIS concentrations. Importantly, TFIIS alone in the absence of RNAPII did not produce any transcript cleavage (Fig. 4*a*, *IIS* lanes).

The effect of TFIIS observed in Fig. 4*a* could be due to either TFIIS preventing incorporation of nucleotide opposite the lesion or the stimulation of transcript cleavage following nucleotide incorporation. To address this issue, we carried out another experiment using an RNA primer with a cytosine opposite the *N*²-Et-dG or dG and incubation in the presence of rNTPs. As shown in Fig. 4*b*, in the absence of TFIIS, small amounts of extension products are visible with the *N*²-Et-dG template. However, with increasing TFIIS concentrations, the amount of extension is reduced, with the concomitant appearance of a product 1 nucleotide shorter than the original primer (Fig. 4*b*). This result indicates that even in the presence of rNTPs, TFIIS stimulates the removal of CMP incorporated opposite the lesion.

To determine the extent of TFIIS-stimulated transcript cleavage, we repeated the experiment shown in Fig. 4*b* in the absence of rNTPs (Fig. 4*c*). Under these conditions, we observed the appearance of an additional TFIIS-

dependent band 2 nucleotides shorter than the starting RNA primer, with both the control and lesion-containing templates. This observation is consistent with others showing that TFIIS stimulated cleavage of transcription complexes stalled because of the absence of rNTPs occurs in dinucleotide increments (38).

Taken together, these results indicate that TFIIS does not act as a bypass factor for transcription past *N*²-Et-dG by mammalian RNAPII. Rather, the TFIIS-induced cleavage activity reduced the steady-state level of nucleoside incorporation opposite the lesion.

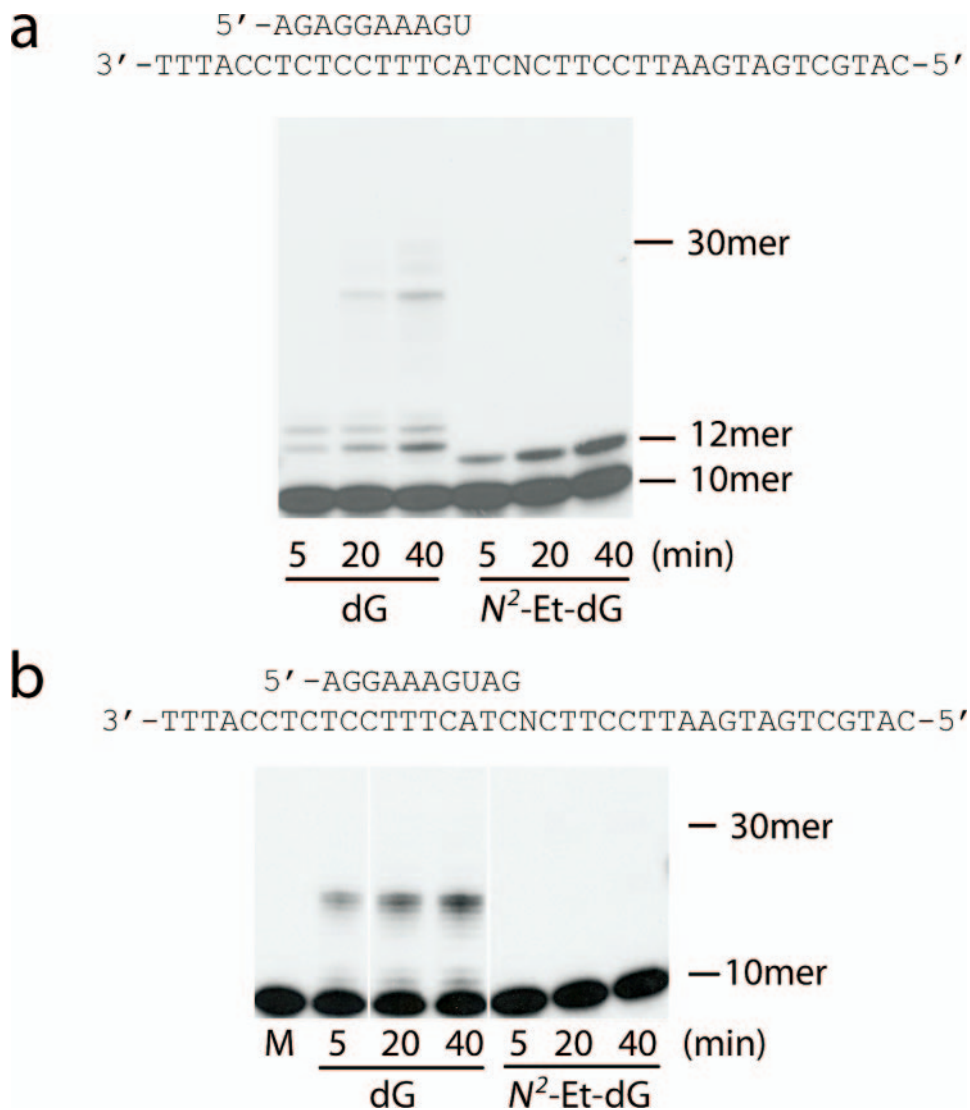


FIGURE 5. The single subunit T7 RNAP cannot insert a nucleotide opposite the *N*²-Et-dG, under running start (a) or standing start (b) conditions. In b, the order of the lanes as shown was electronically modified (white lines) to compensate for a sample loading error. All of the lanes in b were from the same film exposure of the same gel processed identically.

The N²-Et-dG Lesion Blocks Nucleotide Incorporation by T7 RNAP—As mentioned earlier, the mitochondrial localization of ALDH2 indicates that ACD can enter the mitochondrion and therefore might adduct mitochondrial DNA, especially in ALDH2-deficient individuals. To evaluate the blockage effect of the lesion on mitochondrial DNA transcription, we used T7 RNAP as a model enzyme, based on its homology to mitochondrial RNAP. The T7 reactions were conducted in a similar fashion as reactions employing the multisubunit RNAPs.

Under running start conditions, transcription of the *N*²-Et-dG template by T7 RNAP results in a 12-mer. However, in contrast to the results using multisubunit RNAPs (Fig. 2), no 13-mer product resulting from nucleotide incorporation opposite the lesion is detectable under these conditions (Fig. 5a). Consistent with this result, we were also unable to detect nucleotide incorporation opposite the lesion in the standing start set-up (Fig. 5b), although with

very long film exposures, some bypass transcripts can be detected (data not shown).

DISCUSSION

We provide herein data that show that the ACD-derived DNA lesion *N*²-Et-dG is a strong block to both multisubunit and single-subunit RNAPs. Mammalian RNAPII, as well as two other multisubunit RNAPs, are able to slowly incorporate a nucleoside opposite the *N*²-Et-dG lesion, whereas further transcription is strongly inhibited. Thus, the lesion interferes with transcription at both the incorporation and extension steps. Experiments using single rNTPs showed that mammalian RNAPII exclusively incorporates CMP opposite a *N*²-Et-dG lesion, which is a non-mutagenic event, but the incorporation of CMP opposite *N*²-Et-dG is reduced by a factor of ≈ 1500 compared with incorporation opposite dG. In contrast to the multisubunit RNAPs, the single-subunit T7 RNAP is unable to incorporate any rNTP opposite the lesion. Together, these results indicate that the *N*²-Et-dG lesion is a strong block to transcription by both multisubunit and single-subunit RNAPs.

Our results can be compared with published studies of the effects of *N*²-Et-dG on DNA polymerases. With regard to the replicative DNA polymerase α , for which *N*²-Et-dG was shown to be a strong blocking lesion, the only nucleotide that was incorporated opposite the lesion was dCMP, a nonmutagenic event (16). However, during DNA replication, the cells have available a variety of specialized DNA polymerases that can bypass replication blocking DNA lesions (39). With regard to *N*²-Et-dG, the translesion polymerase η as well as other polymerases can bypass *N*²-Et-dG, incorporating dCMP in the process (16, 19, 20). Thus, during replication, polymerase switching is likely to mitigate arrested replication resulting from *N*²-Et-dG *in vivo*.

In contrast, RNAPs are exclusively processive enzymes; specialized translesion RNAPs analogous to DNA polymerase η do not exist. When encountering obstacles to transcription, RNAPs do have accessory elongation factors available that can stimulate bypass in some cases (22, 23). However, our results indicate that the association of TFIIS with RNAPII stalled at an *N*²-Et-dG will not stimulate transcription past the lesion, but in fact accentuates the transcription blocking effect by stimulating transcript cleavage. Thus, although the initial effect of

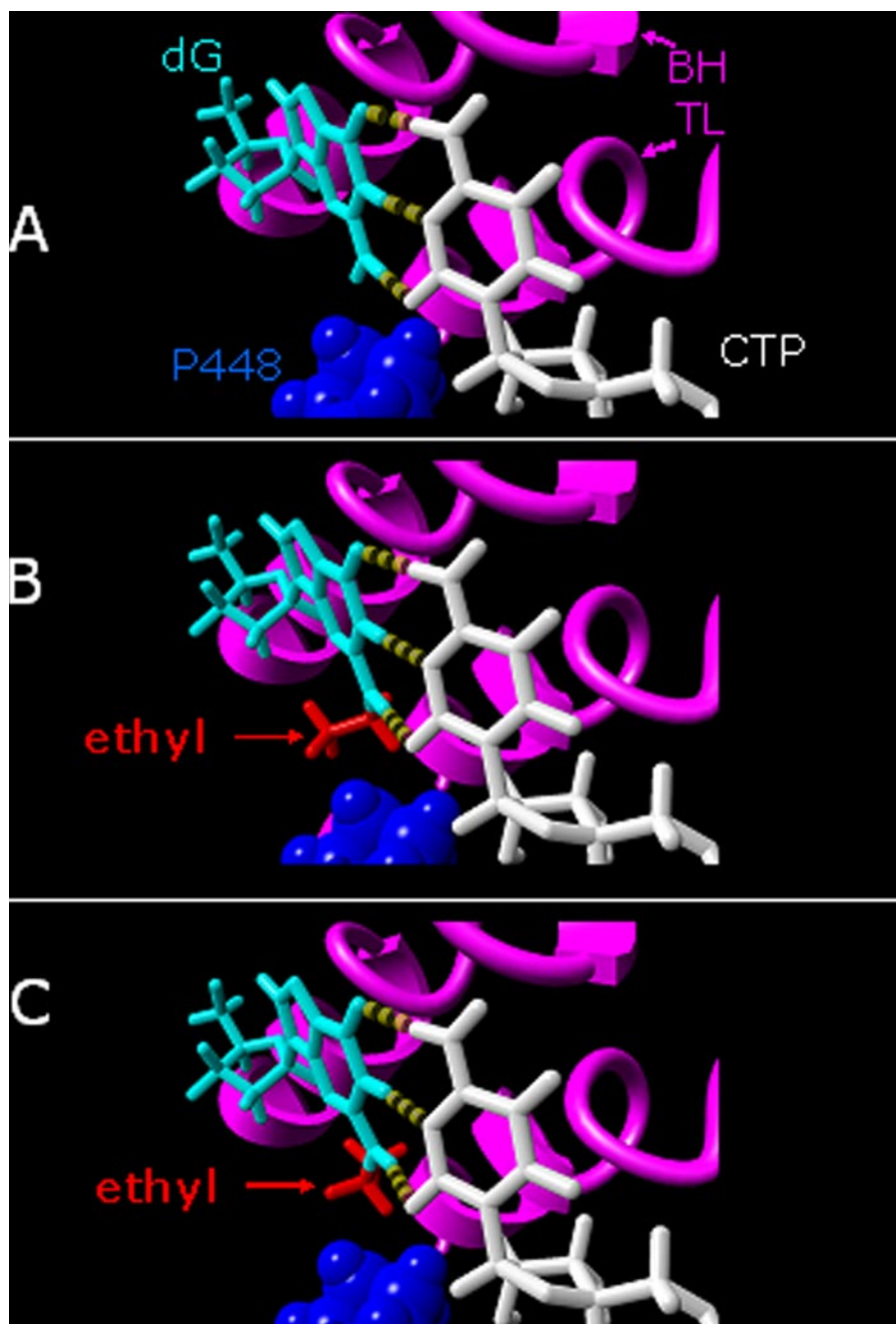


FIGURE 6. Energy-minimized models of the active site yeast RNAPII with a template dG (A) or different configurations of N^2 -Et-dG (B and C) base paired to an incoming CTP. The amino acid residue most likely to clash with some configurations of the ethyl group N^2 -Et-dG is Rpb1 Pro⁴⁴⁸. The two different configurations of the ethyl group within the active site shown in B and C avoid a clash between the lesion and Pro⁴⁴⁸ or any other amino acid within the active site, while allowing three H-bonds (dashed lines) between the template G and incoming CTP. Additional abbreviations: BH, bridge helix; TL, trigger loop. Energy minimization and modeling were done using YASARA-WHAT-IF (28). For additional information about the modeling, see supplementary text.

N^2 -Et-dG on transcription and replication is similar (*i.e.* polymerase blocking in both cases), the effects of the subsequent cellular responses to the blocked polymerases are likely to be very different.

Biological Considerations—Our results using a minimal system demonstrate that N^2 -Et-dG is a strong block to transcription. However, *in vivo*, the ultimate effect of the lesion will depend upon the efficiency of DNA repair, as well as accessory

factors that modulate the effect of the lesion on transcription. With regard to repair, we have been unable to detect cleavage of oligonucleotides containing of N^2 -Et-dG by whole cell extracts from rat liver, under conditions in which glycosylase activity toward uracil, 8-oxo-dG, and ethenoadenine were readily observed.³ These negative results argue against the possibility that N^2 -Et-dG is a substrate for glycosylase initiated BER. Likewise, we found that N^2 -Et-dG is not a substrate for the *E. coli* direct repair enzyme AlkB (40). Although the eukaryotic AlkB homologs were not tested, they show only weak activity against ethylated bases (40). Finally, the absence of mismatch repair had no detectable effect on the genotoxicity of N^2 -Et-dG replicated in human cells (41). Thus, at present, the repair pathway responsible for the repair of N^2 -Et-dG, if any, remains to be elucidated. Also, it is important to bear in mind that our experiments are done with N^2 -Et-dG, whereas the initial lesion formed *in vivo* is N^2 -Eti-dG. N^2 -Et-dG itself is, however, detectable in the human body after ethanol consumption (15).

Turning to the question of transcription bypass factors, we initially tested the ability of TFIIIS to stimulate transcription bypass past N^2 -Et-dG in part because it has been shown that TFIIIS can stimulate transcription past another guanine lesion, 8-oxo-dG (22, 23). Although we found that TFIIIS does not stimulate transcriptional bypass past N^2 -Et-dG, we note that TFIIIS is also not able to stimulate transcription past a different DNA lesion, thymine glycol. However, the Cockayne syndrome B protein, Elongin, and TFIIIF are all able to stimulate transcription past thymine glycol

(22). Thus, it remains possible that one of these factors can stimulate transcription past N^2 -Et-dG *in vivo*. Additional studies will be necessary to test this possibility.

The mitochondrial localization of ALDH2 indicates that ACD can enter the mitochondrion and therefore might accu-

³ P. J. Brooks, unpublished observations.

mutate in mitochondrial DNA, especially in ALDH2-deficient individuals. We used T7 RNAP as a model for mitochondrial RNAP, in an effort to address the possible effects of the N^2 -Et-dG in mitochondria. Our observation that N^2 -Et-dG is an essentially complete block to T7 RNAP *in vitro* suggests that, to the extent that this lesion is formed in mitochondrial DNA *in vivo*, it could impede mitochondrial gene expression and therefore interfere with mitochondrial function. In fact, in preliminary results we have found that N^2 -Et-dG also blocks transcription by purified histidine-tagged yeast mitochondrial RNAP.⁴ Because the liver is the primary site of alcohol metabolism to acetaldehyde (by alcohol dehydrogenase) and ALDH2-deficient individuals are known to have higher levels of N^2 -Et-dG in cellular DNA after alcohol consumption (15), the inhibition of mitochondrial RNA transcription might be especially significant in the liver of ALDH2-deficient individuals after alcohol consumption.

The Function of TFIIS during Transcription at an N^2 -Et-dG Lesion—On nondamaged DNA templates, the two major roles for TFIIS that have been identified are stimulation of transcription elongation and as a transcript cleavage stimulatory factor (34). Likewise, at sites of DNA damage, TFIIS can either stimulate transcript cleavage (36, 37) or act as a bypass factor (22, 23). Our results clearly demonstrate that at N^2 -Et-dG, TFIIS does not act as a bypass factor; rather, it stimulates transcript cleavage and in doing so contributes to the transcription blocking effect of the lesion.

Hawley and co-workers (42) proposed a kinetic partitioning model to explain the proofreading function of TFIIS in which the slow extension of elongation from a mismatched terminus allows time for TFIIS to stimulate cleavage. During the resynthesis step after transcription cleavage, correct nucleotide incorporation allows transcription to continue. Crystal structures of yeast TFIIS complexed with RNAPII are consistent with this model (43).

Our observations on the effect of N^2 -Et-dG can be understood in the context of an analogous model. In essence, the slow incorporation of CMP opposite the lesion, and slow extension of the rC: N^2 -Et-dG base pair allows time for TFIIS to stimulate transcript cleavage analogous to the proofreading model. However, in contrast to the proofreading model, during the resynthesis step following transcript cleavage, the polymerase reincorporates CMP opposite the lesion, again triggering TFIIS-stimulated transcript cleavage. The net result in the presence of TFIIS is a futile cycle of CMP incorporation, transcript cleavage, and resynthesis, resulting in a steady-state condition of polymerase stalling 1 nucleotide before the lesion (Fig. 4a).

Structural Considerations—Dimitri *et al.* (44) recently tested the ability of 1, N^2 -ethnoganine to affect transcription of human RNAPII (in a HeLa nuclear extract) and T7 RNAP. These authors found that 1, N^2 -ethnoganine was a complete block to human RNAPII, whereas T7 RNAP could bypass the lesion. These results are somewhat the opposite of what we found with N^2 -Et-dG. However, the differences can likely be

explained by the different structural effects of the lesion. In 1, N^2 -ethnoganine, the modification is an etheno group with covalent bonds between both N^2 and C-1 of the purine ring. This results in an additional ring to the purine, which blocks access to the active site of RNAPII. In contrast, in N^2 -Et-dG the ethyl group is attached to the N^2 via a single bond. As such, the ethyl group hangs below the guanine base and can therefore potentially adopt a number of different configurations within this space.

Modeling the effect of N^2 -Et-dG on transcription by T7RNAP is complicated by the large structural difference between the open and closed configurations of this enzyme (45, 46). Our current results do not allow us to determine whether the blocking effect of the lesion on transcription takes place in the open or closed states, and therefore we have not attempted to model these possibilities until additional data are available.

Regarding RNAPII, our observations indicate that within the active site the ethyl group in N^2 -Et-dG can adopt one or more configurations that are compatible with the incorporation of CMP opposite the lesion. Using molecular modeling, we have been able to identify multiple configurations of the ethyl group within the polymerase that are compatible with hydrogen bonding between the guanosine base and the cytosine of an incoming CTP. Two examples are shown in Fig. 6. The multiple distinct possible configurations of N^2 -Et-dG in the active site may also provide insight into why we see some bypass of the lesion in the standing start experiments but not in the running start.

Specifically, it may be the case that some configurations of the ethyl group in the active site are compatible with both CMP incorporation and subsequent extension, whereas other configurations of the ethyl group allow CMP incorporation but inhibit subsequent extension. If so, it is possible that configurations that are compatible with subsequent extension might be disfavored under running start conditions compared with the standing start, because of either occupancy of the active site or other locations of the polymerase by rNTPs (47), allosteric effects of rNTPs (48–51), or different configurations of the trigger loop (27, 52). Ultimately, determination of the location(s) of the ethyl group with the active site of the enzyme will require direct structural analysis using x-ray crystallography.

Acknowledgment—We thank Cheryl Marietta for helpful comments on the text.

REFERENCES

- Dellarco, V. L. (1988) *Mutat. Res.* **195**, 1–20
- Baan, R., Straif, K., Grosse, Y., Secretan, B., El Ghissassi, F., Bouvard, V., Altieri, A., and Coglian, V. (2007) *Lancet Oncol.* **8**, 292–293
- Ogawa, H., Gomi, T., and Fujioka, M. (2000) *Int. J. Biochem. Cell Biol.* **32**, 289–301
- Crabb, D. W., Matsumoto, M., Chang, D., and You, M. (2004) *Proc. Nutr. Soc.* **63**, 49–63
- Fraenkel-Conrat, H., and Singer, B. (1988) *Proc. Natl. Acad. Sci. U. S. A.* **85**, 3758–3761
- Vaca, C. E., Fang, J. L., and Schweda, E. K. (1995) *Chem. Biol. Interact.* **98**, 51–67
- Fang, J. L., and Vaca, C. E. (1997) *Carcinogenesis* **18**, 627–632
- Hecht, S. S., McIntee, E. J., and Wang, M. (2001) *Toxicology* **166**, 31–36

⁴ T.-F. Cheng, J. Abraham, and P. J. Brooks, unpublished observations.

Acetaldehyde DNA Lesion Blocks Transcription

9. Wang, M., McIntee, E. J., Cheng, G., Shi, Y., Villalta, P. W., and Hecht, S. S. (2000) *Chem. Res. Toxicol.* **13**, 1149–1157
10. Chen, L., Wang, M., Villalta, P. W., Luo, X., Feuer, R., Jensen, J., Hatsukami, D. K., and Hecht, S. S. (2007) *Chem. Res. Toxicol.* **20**, 108–113
11. Wang, M., Yu, N., Chen, L., Villalta, P. W., Hochalter, J. B., and Hecht, S. S. (2006) *Chem. Res. Toxicol.* **19**, 319–324
12. Brooks, P. J., and Theruvathu, J. A. (2005) *Alcohol* **35**, 187–193
13. Inagaki, S., Esaka, Y., Goto, M., Deyashiki, Y., and Sako, M. (2004) *Biol. Pharm. Bull.* **27**, 273–276
14. Theruvathu, J. A., Jaruga, P., Nath, R. G., Dizdaroglu, M., and Brooks, P. J. (2005) *Nucleic Acids Res.* **33**, 3513–3520
15. Matsuda, T., Yabushita, H., Kanaly, R. A., Shibutani, S., and Yokoyama, A. (2006) *Chem. Res. Toxicol.* **19**, 1374–1378
16. Perrino, F. W., Blans, P., Harvey, S., Gelhaus, S. L., McGrath, C., Akman, S. A., Jenkins, G. S., LaCourse, W. R., and Fishbein, J. C. (2003) *Chem. Res. Toxicol.* **16**, 1616–1623
17. Choi, J. Y., and Guengerich, F. P. (2005) *J. Mol. Biol.* **352**, 72–90
18. Matsuda, T., Terashima, I., Matsumoto, Y., Yabushita, H., Matsui, S., and Shibutani, S. (1999) *Biochemistry* **38**, 929–935
19. Choi, J. Y., Angel, K. C., and Guengerich, F. P. (2006) *J. Biol. Chem.* **281**, 21062–21072
20. Choi, J. Y., and Guengerich, F. P. (2006) *J. Biol. Chem.* **281**, 12315–12324
21. Upton, D. C., Wang, X., Blans, P., Perrino, F. W., Fishbein, J. C., and Akman, S. A. (2006) *Mutat. Res.* **599**, 1–10
22. Charlet-Berguerand, N., Feuerhahn, S., Kong, S. E., Ziserman, H., Conaway, J. W., Conaway, R., and Egly, J. M. (2006) *EMBO J.* **25**, 5481–5491
23. Kuraoka, I., Suzuki, K., Ito, S., Hayashida, M., Kwei, J. S., Ikegami, T., Handa, H., Nakabeppu, Y., and Tanaka, K. (2007) *DNA Repair (Amst.)* **6**, 841–851
24. Masters, B. S., Stohl, L. L., and Clayton, D. A. (1987) *Cell* **51**, 89–99
25. Hu, X., Malik, S., Negroiu, C. C., Hubbard, K., Velalar, C. N., Hampton, B., Grosu, D., Catalano, J., Roeder, R. G., and Gnatt, A. (2006) *Proc. Natl. Acad. Sci. U. S. A.* **103**, 9506–9511
26. Komissarova, N., Kireeva, M. L., Becker, J., Sidorenkov, I., and Kashlev, M. (2003) *Methods Enzymol.* **371**, 233–251
27. Wang, D., Bushnell, D. A., Westover, K. D., Kaplan, C. D., and Kornberg, R. D. (2006) *Cell* **127**, 941–954
28. Vriend, G. (1990) *J. Mol. Graph.* **8**, 52–56
29. Kashkina, E., Anikin, M., Brueckner, F., Pomerantz, R. T., McAllister, W. T., Cramer, P., and Temiakov, D. (2006) *Mol. Cell* **24**, 257–266
30. Pomerantz, R. T., Temiakov, D., Anikin, M., Vassilyev, D. G., and McAllister, W. T. (2006) *Mol. Cell* **24**, 245–255
31. Kireeva, M. L., Komissarova, N., Waugh, D. S., and Kashlev, M. (2000) *J. Biol. Chem.* **275**, 6530–6536
32. Gnatt, A., Fu, J., and Kornberg, R. D. (1997) *J. Biol. Chem.* **272**, 30799–30805
33. Svetlov, V., Vassilyev, D. G., and Artsimovitch, I. (2004) *J. Biol. Chem.* **279**, 38087–38090
34. Fish, R. N., and Kane, C. M. (2002) *Biochim. Biophys. Acta* **1577**, 287–307
35. Wind, M., and Reines, D. (2000) *Bioessays* **22**, 327–336
36. Donahue, B. A., Yin, S., Taylor, J. S., Reines, D., and Hanawalt, P. C. (1994) *Proc. Natl. Acad. Sci. U. S. A.* **91**, 8502–8506
37. Tornaletti, S. (2005) *Mutat. Res.* **577**, 131–145
38. Izban, M. G., and Luse, D. S. (1993) *J. Biol. Chem.* **268**, 12874–12885
39. Prakash, S., Johnson, R. E., and Prakash, L. (2005) *Annu. Rev. Biochem.* **74**, 317–353
40. Koivisto, P., Robins, P., Lindahl, T., and Sedgwick, B. (2004) *J. Biol. Chem.* **279**, 40470–40474
41. Upton, D. C., Wang, X., Blans, P., Perrino, F. W., Fishbein, J. C., and Akman, S. A. (2006) *Chem. Res. Toxicol.* **19**, 960–967
42. Thomas, M. J., Platas, A. A., and Hawley, D. K. (1998) *Cell* **93**, 627–637
43. Kettenberger, H., Armache, K. J., and Cramer, P. (2003) *Cell* **114**, 347–357
44. Dimitri, A., Goodenough, A. K., Guengerich, F. P., Brody, S., and Scicchitano, D. A. (2008) *J. Mol. Biol.* **375**, 353–366
45. Yin, Y. W., and Steitz, T. A. (2004) *Cell* **116**, 393–404
46. Temiakov, D., Patlan, V., Anikin, M., McAllister, W. T., Yokoyama, S., and Vassilyev, D. G. (2004) *Cell* **116**, 381–391
47. Westover, K. D., Bushnell, D. A., and Kornberg, R. D. (2004) *Cell* **119**, 481–489
48. Foster, J. E., Holmes, S. F., and Erie, D. A. (2001) *Cell* **106**, 243–252
49. Holmes, S. F., and Erie, D. A. (2003) *J. Biol. Chem.* **278**, 35597–35608
50. Nedialkov, Y. A., Gong, X. Q., Hovde, S. L., Yamaguchi, Y., Handa, H., Geiger, J. H., Yan, H., and Burton, Z. F. (2003) *J. Biol. Chem.* **278**, 18303–18312
51. Zhang, C., and Burton, Z. F. (2004) *J. Mol. Biol.* **342**, 1085–1099
52. Vassilyev, D. G., Vassilyeva, M. N., Zhang, J., Palangat, M., Artsimovitch, I., and Landick, R. (2007) *Nature* **448**, 163–168